SCIENCE CHINA
Information Sciences

• RESEARCH PAPER •
Special Focus

January 2012 Vol. 55 No. 1: 43–48
doi: 10.1007/s11432-011-4491-5

Angular distribution of terahertz emission from laser interactions with solid targets

DU Fei[1], LI Chun[1], ZHOU MuLin[1], WANG WeiMin[1], SU LuNing[1], ZHENG Yi[1], GE XuLei[1], LI YuTong[1*], MA JingLong[1], LIU XiaoLong[1], ZHANG Lu[1], SHENG ZhengMing[1,2], CHEN LiMing[1], LU Xin[1], DONG QuanLi[1], WANG ZhaoHua[1], WEI ZhiYi[1] & ZHANG Jie[1,2*]

[1] *Beijing National Laboratory of Condensed Matter Physics, Institute of Physics, Chinese Academy of Sciences, Beijing* 100190*, China;*
[2] *Key Laboratory for Laser Plasmas (Ministry of Education) and Department of Physics, Shanghai Jiao Tong University, Shanghai* 200240*, China*

Received July 25, 2011; accepted August 30, 2011

Abstract Intense femtosecond laser-plasma interactions can produce high power terahertz radiations. In our experiment, the polished copper target was irradiated by a p-polarized laser with intensity of more than 10^{18} W/cm^2 at an incident angle of 67.5° from the target normal. The THz energy from three different detection angles is measured. The maximum emission is found in the direction at an angle of 45° to the laser backward direction, which is more than one order of magnitude higher than in the other two directions. A simple theoretical model has been established to explain the measurements.

Keywords terahertz emission, laser solid interactions, angular distribution

Citation Du F, Li C, Zhou M L, et al. Angular distribution of terahertz emission from laser interactions with solid targets. Sci China Inf Sci, 2012, 55: 43–48, doi: 10.1007/s11432-011-4491-5

1 Introduction

Terahertz (THz) radiation has wide-range applications in many different domains, such as semiconductor [1,2], biomedical [3,4], imaging [5,6], etc., because of its unique characteristics. Two conventional methods, photoconductive switches [7–9] and optical rectification [10], are used to generate broadband pulsed THz emission. Limited by the material damage threshold, the THz emission energy cannot be further increased by applying higher intensity laser. There are two new candidates for generating high power THz radiation. One is accelerator-based radiation, such as coherent synchrotron radiation [11,12], coherent transition radiation [13], free electron laser [14], Cherenkov radiation [15] and Smith-Purcell effect [16], etc. These facilities can provide a high average power output tunable at a very broad band. The other is laser-produced plasmas. The phenomenon that a laser produced air filament emits THz wave has recently been reported [17] and a series of improvements are employed [18,19]. However, the laser intensity still

*Corresponding author (email: ytli@aphy.iphy.ac.cn, jzhang1@sjtu.edu.cn)

cannot be too high in air as a result of some complex nonlinear effects. In vacuum, the laser can interact with high density matter at an ultrahigh intensity, generating particles and photons with different energy. Leemans et al. have reported that laser accelerated electron bunches can generate THz emission at the plasma-vacuum boundary [20]. With solid target, powerful THz sources have also been obtained [21], demonstrating a promising future although its generation mechanism is still not fully understood.

In our recent work, we have obtained a THz energy as high as 50 μJ/sr per shot and discussed the effect of the laser contrast ratio1) [22]. In this paper, we will present the measurement of the angular distribution of the THz radiation and discuss the THz generation mechanism.

2 Experimental setup

The experiments were performed at XL-II (Xtreme Light II) 20 TW Ti: Sapphire laser facility which provided an 800 nm, 70 fs laser pulse. Through an f/3.5 off-axis parabolic mirror, a *p*-polarized laser with an amplified spontaneous emission (ASE) contrast ratio of $\sim 10^{-7}$ was focused onto a 10 mm×20 mm× 1 mm copper target with an incidence angle of 67.5° to the target normal. The full width at half maximum (FWHM) of the focal spot was 5 μm. It contained 35% of total pulse energy, monitored and measured by a microscopic system and a beam profile analysis system. With the pulse energy of 180 mJ, the laser intensity was 4.6×10^{18} W/cm^2. The target surface was polished before equipped in the vacuum chamber. After each shot the target was moved by 300 μm, the laser pulse was made to irradiate a fresh target region.

The experimental setup is shown in Figure 1. There were four diagnostic channels in our experiment, three for THz emission and one for visible light. The optic system of channel 1 to 3 was constituted by polymethylpentene (TPX) lenses and windows and that of channel 4 by glass. Channel 1 and 2 were almost the same but the collecting angle to the target normal. They had only one TPX lens responsible for collecting the emitted THz wave and focusing it onto the detector through a TPX window outside the vacuum chamber. The angle between the central THz wave path and target normal was −22.5° (channel 1) and 22.5° (channel 2), where the minus sign means the path direction and the laser beam are on the same quadrant (the minus quadrant). Before THz wave enters the detector, there will be one or more high resistivity float zone silicon plates (HRFZ-Si) placed in front of the crystal in order to screen off the visible light and extenuate the THz emission when it was so intense that the electric signal from the detector was saturated. The collecting solid angle of the TPX lenses was 0.021 (see Table 1). In channel 3, the focal point of the TPX lens was exactly put on the target point, so the THz wave was first collimated, passed through the TPX window and was refocused onto the detector by another TPX lens. The central path of channel 3 was 67.5° to the target normal, with a solid angle of 0.036°. An $LiTaO_3$ pyroelectric detector was used to measure the power of the THz emission, with a relative flat broadband response from 0.1 to 30 THz. In order to collect almost all the emissions from each channel, a copper cone was used in front of the crystal of the detector. Channel 4 was composed of an optical glass lens and a window. The visible light was focused onto a fiber spectrometer with spectrum response from 200 to 1100 nm to monitor the second and three-half harmonic. The detailed information of these 4 channels is given in Table 1. There was an NaI γ-ray detector 120 cm away from the target, measuring the high energy photons above 0.15 MeV. With all these detection systems, we can measure the electromagnetic radiation from the plasma with a very broad range from gamma ray to THz.

3 Experimental results and discussions

The typical visible light spectrum is shown in Figure 2. We can see the obvious 3/2 harmonic at 533 nm and relatively weak second harmonic at 400 nm. This is in good agreement with our previous experimental

1) Li Y T, Li C, Zhou M L, et al. Strong terahertz radiation from relativistic laser interaction with solid density plasmas, submitted

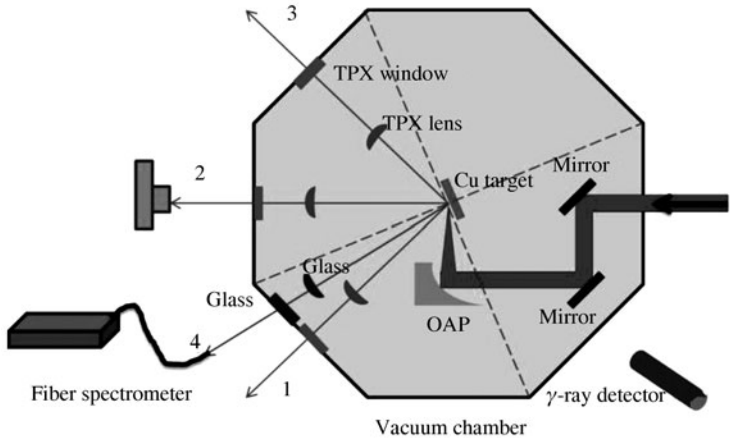

Figure 1 Schematic of the experimental setup. There are 4 detection channels, 1 to 3 for angular distribution of the THz emission and 4 for the visible light spectrum. A NaI detector is responsible for high energy γ-ray real-time monitoring. The blue dashed lines give the direction of the target normal and the surface, respectively.

Table 1 Parameters of detection channels

Channel	Angle(°)	Solid angle (sr)	Detector
1	−22.5	0.020	pyroelectric
2	22.5	0.021	pyroelectric
3	67.5	0.036	pyroelectric
4	−7.5	0.016	fiber spectrometer

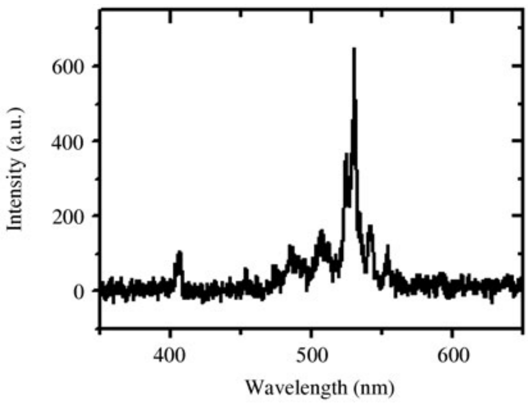

Figure 2 Visible light spectrum at channel 4. With the ASE contrast ratio of $\sim 10^{-7}$, 3/2 harmonic is much stronger than the second harmonic.

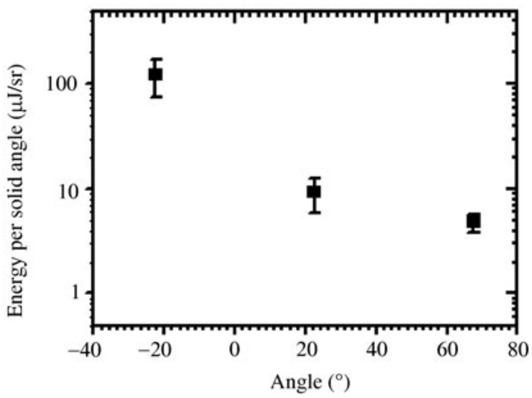

Figure 3 The THz energy for the three directions of −22.5°, 22.5° and 67.5°.

and theoretical results under this ASE contrast ratio condition [22].

At each THz radiation detection angle, at least 6 efficient shot data was recorded. Taking into account the transmittance of the TPX lenses, windows and HRFZ-Si extenuator, the absolute energy of THz emission from laser-solid targets interaction is calculated. Normalized by the collecting solid angle, we can get 122.8, 9.3, 4.8 μJ/sr at −22.5°, 22.5°, 67.5°, respectively (see Figure 3). The highest energy is observed at −22.5°, about one order of magnitude higher than the other two directions. On the contrary, the THz emission in the specular reflection direction in our experiment is the weakest.

To understand the above experimental results, we establish a new self-organized fast electron current model to shed light on the mechanism of THz generation[1)]. We believe that the THz emission is attributable to the fast electron current along the target surface. Considering that the dimension of the interaction area is only around 10 μm, we ignore the current density distribution for simplicity. So it can

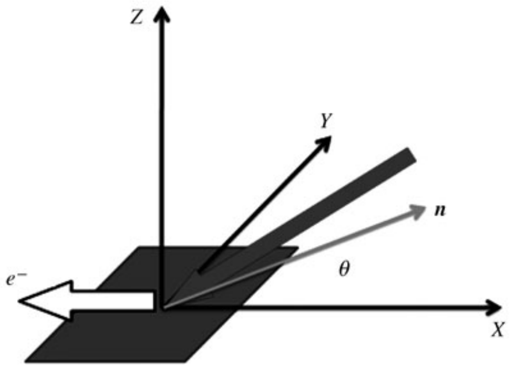

Figure 4 Coordinates of the model. The laser irradiates the target in the XOZ plane. Z axis is also the target normal. The transient electrons are moving opposite to the X direction, producing a positive current. $\boldsymbol{n}$ is the unit direction vector from the current center to the detector, with angle θ to the X axis.

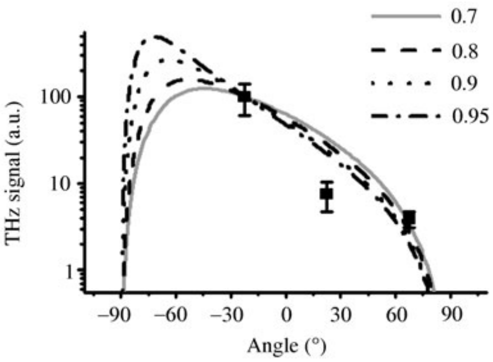

Figure 5 The expected angular distribution of the self-organized fast electron current model. Four different β are used to investigate the influence of the surface electron velocity. They are all normalized at the angle $-22.5°$ for comparison. The measured data are also depicted in the figure, showing a similar tendency with the model.

be assumed as a point current, $J = J_0\delta(\boldsymbol{r})\exp(-t^2/\tau_0^2)$, where τ_0 is a constant determined by the laser pulse duration. The schematic of the model coordinates is shown in Figure 4.

For the electrons flowing along the target surface [23], the transient current can be written as $\boldsymbol{J} = \boldsymbol{e}_x J_0\delta(\boldsymbol{r})\exp(-t^2/\tau_0^2)$, where J_0 is proportional to the laser intensity I_0. The detection direction vector is $\boldsymbol{n}$. Substituting the current form into the retarded potential formula, we can get

$$\boldsymbol{A}(t) = \int \frac{\boldsymbol{J}(t-R/c)}{cR}\mathrm{d}V' = \frac{1}{cR_0}\int \boldsymbol{J}(t-R/c)\mathrm{d}V' = \frac{\boldsymbol{e}J_0\exp(-t^2/\tau_0^2)}{cR_0}. \tag{1}$$

By using the far filed approximation, the distance between the detector and the emission source, R_0 can be assumed as a constant. As the detector is small enough, the electromagnetic wave at the detector can be considered as a plane wave, $\boldsymbol{E} = \boldsymbol{H}\times\boldsymbol{n}$ and $\boldsymbol{H} = \frac{1}{c}\frac{\partial \boldsymbol{A}(t)}{\partial t}\times\boldsymbol{n}$. After a series of calculations, we can obtain the formula of the electric field of the THz emission at the detector:

$$\boldsymbol{E} = \frac{2J_0 t\exp(-t^2/\tau_0^2)}{c^2\tau_0^2 R_0(1-\boldsymbol{n}\cdot\boldsymbol{\beta})}\boldsymbol{n}\times(\boldsymbol{n}\times\boldsymbol{e}_x), \tag{2}$$

where $\boldsymbol{\beta}$ is the average normalized velocity of electrons that form the transient current. So we can calculate the angular distribution of the THz energy flow, $\boldsymbol{S} = \frac{\boldsymbol{n}c}{4\pi}\boldsymbol{E}^2$. Normalized by the collecting solid angle, the energy distribution in the laser incident plane is

$$\mathrm{d}P_\Omega/\boldsymbol{d}\Omega = \frac{J_0^2 t^2\exp(-2t^2/\tau_0^2)\sin^2\theta}{\pi c^3\tau_0^4(1-\beta\cos\theta)^2} \propto \frac{\sin^2\theta}{(1-\beta\cos\theta)^2}. \tag{3}$$

Eq. (3) gives the relation between the detection angle and the THz energy per unit solid angle in the laser incident plane.

In Figure 5, we depict the model and the experimental measurement. For comparison, the model line and the measured data are normalized at $-22.5°$. The energy of escaping fast electrons is from hundreds of keV to several MeV [24–27]. The estimated velocity of the electrons which constitute the transient current is comparable to that of the electrons emitted from the target. The parameter β is chosen as 0.7, 0.8, 0.9 or 0.95, representing the electron energy from about 0.2 to 1.1 MeV. Obviously, with the increasing average velocity of the electrons, the maximum emission direction is approaching the current direction. However, the angular distribution is almost insensitive to the velocity of the transient current electrons when the detection angle is in the range of our experiment($> -30°$), demonstrating a similar declining tendency. That tendency shows a good agreement with our measurement. The data at 22.5° deviates a little from the model expectation, probably resulting from the strong simplified assumption of this model. The laser produced plasmas have extremely complicated time and space structures and tremendously variable magnetic and electric environments, in which the moving particles are influenced by many parameters. In order to understand the process more precisely, the transient current intensity and direction distribution should be considered in detail.

4 Conclusion

We have measured the angular distribution of the terahertz emission of laser solid target interactions at -22.5°, 22.5° and 67.5° to the target normal. The THz maximum emission is found at -22.5°. The angular distribution demonstrates an increasing tendency as the detection angle approach the laser backward direction. We establish a simple model by assuming a transient current on the target surface. The model shows a good agreement with our experimental results.

Acknowledgements

This work was supported by the National Natural Science Foundation of China (Grant Nos. 10925421, 10734130).

References

1 Shi Y L, Yang Y P, Xu X L, et al. Ultrafast carrier dynamics in Au/GaAs interfaces studied by terahertz emission spectroscopy. Appl Phys Lett, 2006, 88: 161109
2 Gaal P, Reimann K, Woerner M, et al. Nonlinear terahertz response of n-type GaAs. Phys Rev Lett, 2006, 96: 187402
3 Shen Y C, Upadhya P C, Linfield E H, et al. Temperature-dependent low-frequency vibrational spectra of purine and adenine. Appl Phys Lett, 2003, 82: 2350–2352
4 Siegel P H. Terahertz technology in biology and medicine. IEEE Trans Microw Theory Tech, 2004, 52: 2438–2447
5 Hu B B, Nuss M C. Imaging with terahertz waves. Opt Lett, 1995, 20: 1716
6 Jepsen P U, Cooke D G, Koch M. Terahertz spectroscopy and imaging-modern techniques and applications. Laser Photon Rev, 2011, 5: 124–166
7 Vanexter M, Fattinger C, Grischkowsky D. High-brightness terahertz beams characterized with an ultrafast detector. Appl Phys Lett, 1989, 55: 337–339
8 Zhang X C, Hu B B, Darrow J T, et al. Generation of femtosecond electromagnetic pulses from semiconductor surfaces. Appl Phys Lett, 1990, 56: 1011–1013
9 Gu P, Tani M, Kono S, et al. Study of terahertz radiation from InAs and InSb. J Appl Phys, 2002, 91, 5533–5537
10 Auston D H, Cheung K P, Valdmanis J, et al. Cherenkov radiation from femtosecond optical pulses in electro-optic media. Phys Rev Lett, 1984, 53: 1555–1558
11 Abo-Bakr M, Feikes J, Holldack K, et al. Steady-state far-infrared coherent synchrotron radiation detected at BESSY II. Phys Rev Lett, 2002, 88: 254801
12 Byrd J M, Hao Z, Martin M C, et al. Laser seeding of the storage-ring microbunching instability for high-power coherent terahertz radiation. Phys Rev Lett, 2006, 97: 074802
13 Shen Y, Watanabe T, Arena D A, et al. Nonlinear cross-phase modulation with intense single-cycle terahertz pulses. Phys Rev Lett, 2007, 99: 043901
14 Jaroszynski D A, Bakker R J, Vandermeer A F G, et al. Coherent startup of an infrared free-electron laser. Phys Rev Lett, 1993, 71: 3798–3801
15 Takahashi T, Shibata Y, Ishi K, et al. Observation of coherent Cerenkov radiation from a solid dielectric with short bunches of electrons. Phys Rev E, 2000, 62: 8606–8611
16 Korbly S E, Kesar A S, Sirigiri J R, et al. Observation of frequency-locked coherent terahertz Smith-Purcell radiation. Phys Rev Lett, 2005, 94: 054803
17 Cook D J, Hochstrasser R M. Intense terahertz pulses by four-wave rectification in air. Opt Lett, 2000, 25: 1210–1212
18 Bartel T, Gaal P, Reimann K, et al. Generation of single-cycle THz transients with high electric-field amplitudes. Opt Lett, 2005, 30: 2805–2807
19 Xie X, Dai J M, Zhang X C. Coherent control of THz wave generation in ambient air. Phys Rev Lett, 2006, 96: 075005
20 Leemans W P, Geddes C G R, Faure J, et al. Observation of terahertz emission from a laser-plasma accelerated electron bunch crossing a plasma-vacuum boundary. Phys Rev Lett, 2003, 91: 074802
21 Hamster H, Sullivan A, Gordon S, et al. Subpicosecond, electromagnetic pulses from intense laser-plasma interaction. Phys Rev Lett, 1993, 71: 2725–2728
22 Li C, Zhou M L, Ding W J, et al. Effects of laser-plasma interactions on terahertz radiation from solid targets irradiated by ultrashort intense laser pulses. Phys Rev E, 2011, 84: 036405
23 Li Y T, Yuan X H, Xu M H, et al. Observation of a fast electron beam emitted along the surface of a target irradiated by intense femtosecond laser pulses. Phys Rev Lett, 2006, 96: 165003
24 Beg F N, Bell A R, Dangor A E, et al. A study of picosecond laser-solid interactions up to 10(19) W cm(−2). Phys Plasmas, 1997, 4: 447–457

25 Wharton K B, Hatchett S P, Wilks S C, et al. Experimental measurements of hot electrons generated by ultraintense (>10(19) W/cm(2)) laser-plasma interactions on solid-density targets. Phys Rev Lett, 1998, 81: 822–825

26 Amiranoff F. Fast electron production in ultra-short high-intensity laser-plasma interaction and its consequences. Meas Sci Technol, 2001, 12: 1795–1800

27 Zhang J, Li Y T, Sheng Z M, et al. Generation and propagation of hot electrons in laser-plasmas. Appl Phys B-Lasers Opt, 2005, 80: 957–971

DU Fei was born in 1985. He is now a Ph.D. candidate of Institute of Physics, Chinese Academy of Sciences. He received the Bachelor degree in Physics from Shandong University in 2007. Currently, his research interests is in the generation of terahertz radiation from laser solid target interactons.

SHENG ZhengMing received the degree of Doctor of Science from the Shanghai Institute of Optics and Fine Mechanics, CAS, in 1993. During 1995-1998, he worked in the Max-Planck Institute for Quantum Optics, Garching, as a Humboldt research fellow and the postdoctoral fellow of Max-Planck Society. During 1998-2001 he worked in the Institute of Engineering, Osaka University as the JSPS fellow and researcher of the university. Since 2001 he has been working in the Institute of Physics, CAS, as senior research scientist. Currently he is also the Changjiang professor of Shanghai Jiao Tong University.

LI YuTong is working at the Institute of Physics, Chinese Academy of Sciences. His main research interests include fast electron generation and transport relevant to fast ignition of the Inertial Confinement Fusion, MeV proton and ion generation, strong THz generation, and laboratory astrophysics. From 2000 he and his collaborators have published over 100 papers. His research has been recognized by the Chinese State Council with the Natural Sciences Prize in 2006 and Chinese Physical Society with the Wang Gan Chang Prize in 2011.

ZHANG Jie received his Ph.D. degree in 1988 at the Institute of Physics of the Chinese Academy of Sciences (CAS). Then he joined the Max-Planck-Institute for Quantenoptik in Germany. In 1990-1998, he worked for the Rutherford Appleton Laboratory and the University of Oxford in the UK. Dr. Zhang was elected the President of Association of Asia Pacific Physical Societies (AAPPS) and the member of the German Academy of Sciences Neopoldina in 2007; Academician of the Chinese Academy of Sciences in 2003. He was given TWAS Prize in Physics in 2007; the Natural Sciences Prize in 2006; the Ho Leung Ho Lee award of the Science and Technology Progress Award in 2006; etc.